Environmental Science & Technology

Article

Cite This: Environ. Sci. Technol. 2018, 52, 13089−13098

pubs.acs.org/est

Effect of Calcium on the Bioavailability of Dissolved Uranium(VI) in Plant Roots under Circumneutral pH

Eliane El Hayek,*[,†] Chris Torres,[‡] Lucia Rodriguez-Freire,[§] Johanna M. Blake,[∥] Cherie L. De Vore,[⊥] Adrian J. Brearley,[#] Michael N. Spilde,[#] Stephen Cabaniss,[†] Abdul-Mehdi S. Ali,[#] and José M. Cerrato*[,⊥]

[†]Department of Chemistry and Chemical Biology, MSC03 2060, University of New Mexico, Albuquerque, New Mexico 87131, United States

[‡]Department of Chemical and Biological Engineering, MSC01 1120, University of New Mexico, Albuquerque, New Mexico 87131, United States

[§]Department of Civil and Environmental Engineering, New Jersey Institute of Technology, Newark, New Jersey 07102, United States

[∥]U.S. Geological Survey, 6700 Edith Blvd. NE, Albuquerque, New Mexico 87113, United States

[⊥]Department of Civil Engineering, MSC01 1070, University of New Mexico, Albuquerque, New Mexico 87131, United States

[#]Department of Earth and Planetary Sciences, MSC03 2040, University of New Mexico, Albuquerque, New Mexico 87131, United States

Supporting Information

ABSTRACT: We integrated field measurements, hydroponic experiments, microscopy, and spectroscopy to investigate the effect of Ca(II) on dissolved U(VI) uptake by plants in 1 mM HCO_3^- solutions at circumneutral pH. The accumulation of U in plants (3.1−21.3 mg kg^{-1}) from the stream bank of the Rio Paguate, Jackpile Mine, New Mexico served as a motivation for this study. *Brassica juncea* was the model plant used for the laboratory experiments conducted over a range of U (30−700 $\mu g\ L^{-1}$) and Ca (0−240 mg L^{-1}) concentrations. The initial U uptake followed pseudo-second-order kinetics. The initial U uptake rate (V_0) ranged from 4.4 to 62 $\mu g\ g^{-1}\ h^{-1}$ in experiments with no added Ca and from 0.73 to 2.07 $\mu g\ g^{-1}\ h^{-1}$ in experiments with 12 mg L^{-1} Ca. No measurable U uptake over time was detected for experiments with 240 mg L^{-1} Ca. Ternary Ca−U−CO_3 complexes may affect the decrease in U bioavailability observed in this study. Elemental X-ray mapping using scanning transmission electron microscopy−energy-dispersive spectrometry detected U−P-bearing precipitates within root cell walls in water free of Ca. These results suggest that root interactions with Ca and carbonate in solution affect the bioavailability of U in plants. This study contributes relevant information to applications related to U transport and remediation of contaminated sites.

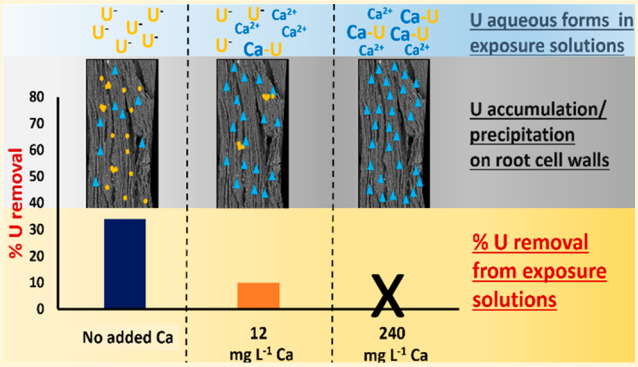

INTRODUCTION

The bioavailability of uranium (U) in contaminated environments has received growing attention because of potential ecological and human health risks from mining, nuclear energy generation, and weapons manufacturing. Improper uranium mine waste disposal remains a global concern because of U contamination of water, soils, and various ecosystems.[1−3] The accumulation of U and other toxic metals in plants has been commonly studied as a potential pathway for human exposures[1,4−6] and for the development of remediation approaches in contaminated sites.[7−9]

This study was conducted in the context of the Jackpile Mine, Laguna Pueblo, New Mexico, which is an example of a mine site affected by U mining legacy. Mining operations at the Jackpile Mine were active from 1953 to 1982.[10,11] Concentrations of U in surface waters from Rio Paguate near the Jackpile Mine have been recently detected above the U.S. Environmental Protection Agency (USEPA) Maximum Contaminant Level (MCL) of 30 $\mu g\ L^{-1}$.[12,13] Given the water chemistry at Rio Paguate (e.g., pH and Ca, U, and carbonate concentrations), aqueous ternary uranyl-carbonate complexes (Ca−U−CO_3) may be an important factor decreasing U interaction with sediments colocated in the stream bed and

Received: May 21, 2018
Revised: October 25, 2018
Accepted: October 29, 2018
Published: November 9, 2018

DOI: 10.1021/acs.est.8b02724
Environ. Sci. Technol. 2018, 52, 13089−13098

bank of Rio Paguate.[14] However, the effects of these Ca−U−CO_3 complexes on U bioavailability in plants at the Jackpile Mine are unknown.

Water chemistry has a major influence on U bioavailability. It is generally understood that an increase in pH, water hardness, alkalinity, and organic colloids reduces U uptake and toxicity.[15−17] Such effects are attributed to either competitive binding−uptake mechanisms at the cell surface (e.g., between the free UO_2^{2+} and H^+, Ca^{2+}) or U speciation through aqueous complexation.[18,19] Most studies consider that the free uranyl ion[20,21] (UO_2^{2+}) and U hydrolysis species[22] are key to U uptake by living systems (e.g., terrestrial plants, invertebrates, algae). Binary and ternary uranyl-carbonate complexes are also relevant in natural waters in which Ca and carbonate are present.[23−26] However, the importance of these uranyl-carbonate complexes has been largely overlooked in the literature for U bioavailability, and the effect of Ca on U toxicity in contaminated waters is not well-understood.[27] A recent study[28] reported that uranyl-carbonate complexes can be an indicator of U uptake rates in invertebrates but that ternary complexes (e.g., $CaUO_2(CO_3)_3^{2-}$) decreased rates of U uptake. Both $Ca_2UO_2(CO_3)_3$ and $CaUO_2(CO_3)_3^{2-}$ complexes can act as nontoxic species in contaminated waters.[29−31] Limited studies have addressed Ca impact on U bioavailability in plants.[18,21,32−34]

The mechanisms for U uptake in plants largely depend on aqueous chemical speciation.[22,35−37] The ion UO_2^{2+} can highly adsorb and/or accumulate in plant roots at low pH and low sulfate and phosphate concentrations.[33,38] Complexation of UO_2^{2+} with carbonate and citrate was found to increase root-to-shoot translocation but to decrease total U accumulation in plants.[33] Inside the plant roots, UO_2^{2+} can precipitate with the endogenous phosphorus as U(VI)-phosphate,[39−41] whereas U citrate can be accumulated as U carboxylate.[39] Under favorable conditions for iron-reducing bacteria, U can be found mainly associated with phosphorus on plant roots in the oxidized U(VI) and the reduced U(IV) forms.[42,43] However, the effects of water chemistry at environmentally relevant conditions (e.g., circumneutral pH, the presence of complexing agents such as carbonate and/or major elements such as Ca and Mg) on the bioavailability and the uptake mechanisms of U by plants are still largely unknown. Information on the mechanisms governing U uptake in plants is important for predicting U mobility and long-term remediation strategies.

The main objective of this study was to assess U bioavailability integrating field measurements, hydroponic experiments, microscopy, and spectroscopy analyses. The accumulation of U was measured in plants collected from the Jackpile Mine, along the Rio Paguate. Hydroponic experiments were conducted in systems containing 1 mM HCO_3^- at pH 7.5, with U and Ca concentrations relevant to water chemistry in the Rio Paguate. *Brassica juncea* (*B. juncea*) was selected as the model organism as it is a known U hyperaccumulator plant.[8,9] Our findings contribute relevant information to better understand the influence of Ca and carbonate on U bioavailability in abandoned mine wastes and other natural sites affected by elevated U concentrations.

MATERIALS AND METHODS

Plant Sampling Locations. Plant samples (shoots and roots) were collected from the stream banks of the Rio Paguate near and within the wetland area up to 5 km downstream of the Jackpile Mine, situated in Figure S1 between sites 1 and 10. The sampling sites of plants were colocated with water and stream bank sediment samples that were studied by Blake et al. during the same time period (Table S1).[14] Regional plants (grass, willow (*Salix*), and cattail (*Typha latifolia L.*)), which are abundant at the site and may be used as cattle fodder or for ceremonial traditions, were sampled (Table S1). Detailed information for the sites and laboratory plant preparation is presented in the Supporting Information.

Growth and Preparation of *Brassica juncea*. After germination, the seedlings of *B. juncea* were allowed to grow in a hydroponic system supplied with NPK liquid fertilizer under 21−25 °C day and night temperature in 12 h/12 h light cycle. Two-month-old seedlings were acclimatized to the exposure conditions for 5 days by placing each one of them separately in 500 mL of Nalgene polypropylene (PP) bottles containing the same elemental composition of the exposure solution but without U. To avoid any possibility of improper U complexation or precipitation (e.g., complexation with phosphate) in the uptake experiments, the exposure solutions were made in ultrapure water containing only simplified Hoagland nutrients ($MgSO_4$, 0.5 mM; NH_4NO_3, 2 mM; KCl, 1 mM; $NaHCO_3$, 1 mM; and $CaCl_2{\cdot}2H_2O$, 3 mM). The measured pH of the acclimatized solution was in the range of 5.8−6.2. More details are presented in the Supporting Information.

Exposure of *Brassica juncea* to U. The effect of Ca on U bioavailability was tested by studying U uptake kinetics at three Ca concentrations (0, 12, and 240 mg L^{-1}) in water containing 1 mM HCO_3^- (alkalinity 50 mg L^{-1}) with pH maintained at 7.5 using 2 mM HEPES buffer. Laboratory controlled experiments were conducted using *B. juncea* as a model system for research investigating U bioaccumulation in plants.[9,44,45] The tested U, Ca, and pH levels correspond to Jackpile Mine conditions[14] (Table S1) and to other environments where binary and ternary uranyl-carbonate complexes are prevalent.[23] Uptake experiments were performed in freshly made solutions prepared in ultrapure water with the same simplified Hoagland nutrients but with changing Ca concentrations (0, 12, and 240 mg L^{-1}) and adding 30, 100, 300, or 700 μg L^{-1} U concentrations as $UO_2(NO_3)_2$. All the experiments were performed in triplicate. Aliquot volumes were collected at various time points (from 4 to 336 h) to assess U uptake kinetics. We also exposed other plant seedlings to 700 μg L^{-1} U at the same conditions described above to assess the kinetics of U uptake during the first hours of U exposure from 0.6 to 24 h. Detailed descriptions about seedling preparation, the composition of exposure solutions, and methods used for U analysis are presented in the Supporting Information.

Solid and Solution Analyses. Total U for hydroponic solutions and acid-digested plant samples were analyzed using inductively coupled-plasma mass-spectrometry (ICP-MS). We used Visual MINTEQ[46,47] to assess U aqueous speciation using inputs based on the experimental conditions used for this study. Statistical analyses were conducted to analyze the significance of the effects of U, Ca, and U × Ca treatments on U uptake by plant roots using the software XLSTAT.[48] Nonparametric tests were performed because of the non-normality of our data sets as determined using the Shapiro−Wilk test. The statistically significant level was set at $\alpha = 0.05$ ($p < 0.05$) for all the statistical tests. Additional details about these statistical methods are presented in the Supporting Information.

Dried root samples were analyzed using scanning electron microscopy (SEM), electron microprobe analysis (EPMA),

DOI: 10.1021/acs.est.8b02724
Environ. Sci. Technol. 2018, 52, 13089−13098

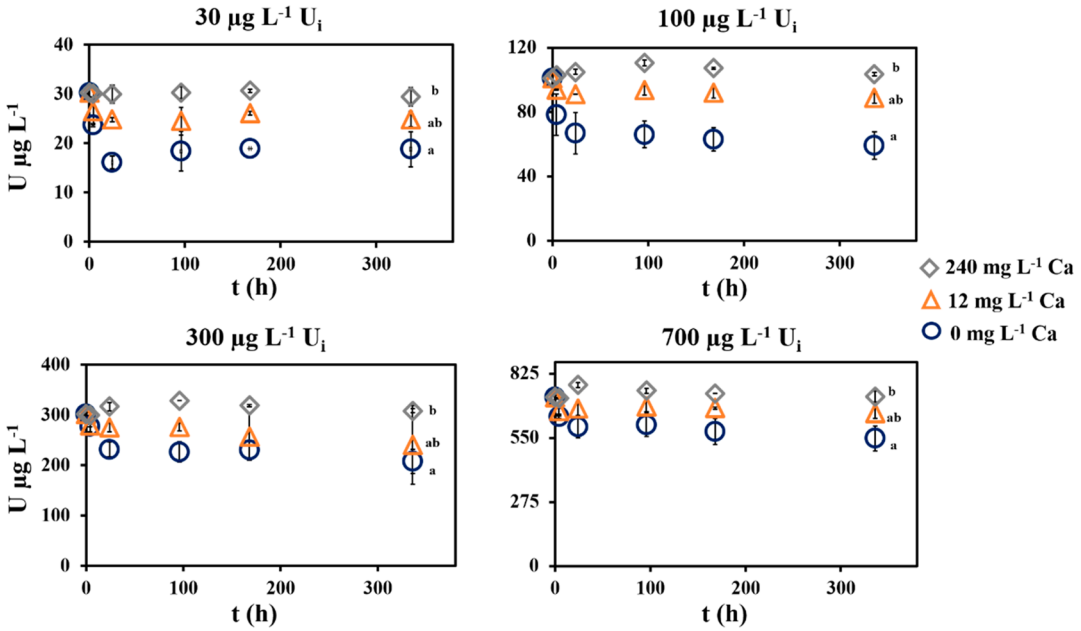

Figure 1. Concentration of U (μg L^{-1}) as a function of reaction time in solutions containing 1 mM HCO_3^- at pH 7.5 at different levels of initial U_i (30, 100, 300, and 700 μg L^{-1}) and Ca (0, 12, and 240 mg L^{-1}) concentrations. The standard deviation was determined from triplicate experiments. Different letters indicate significant difference ($p < 0.05$) in the variation of aqueous U concentration (as indicated by Kruskal–Wallis test followed by Dunn's test) between solutions with different Ca treatments at the different levels of initial U_i concentration.

and focused ion beam-transmission electron microscopy (FIB-TEM) techniques. Additional details describing solution and solid analyses can be found in the Supporting Information.

Kinetic Analyses of Aqueous U. The quantity of U removed in micrograms per gram of dry weight of roots at time t was calculated from the mass balance between the initial concentration in the exposure solution and the measured concentration at different time intervals. Note that the uptake of U by the plant was also confirmed by measuring U content in the digested plant samples at the end of the experiments. Pseudo-second-order kinetic analyses were found to best mathematically represent the uptake of U by *B. juncea* roots in comparison with several kinetic models (first- and second-order and pseudo-first-order) tested on the experimental data. The kinetic equation is

$$dq_t/dt = k_2(q_e - q_t)^2 \quad (1)$$

where k_2 (g μg^{-1} h^{-1}) is the rate constant of pseudo-second-order of metal uptake[49,50] and q_e and q_t represent the mass of U per gram of root tissue (μg g^{-1}) at equilibrium and time t, respectively. Solving and rearranging eq 1 gives

$$t/q_t = 1/V_0 + 1/q_e t \quad (2)$$

where V_0 is the initial uptake rate (μg g^{-1} h^{-1}) and is equal to the following equation:

$$V_0 = k_2 q_e^{\ 2} \quad (3)$$

The values of V_0, k_2, and q_e can be experimentally obtained by plotting t/q_t versus t. Uranium uptake kinetics applied in this study follow a similar approach to the model used for adsorption–absorption mechanisms and metal bioaccumulation by plants and bacteria.[49,51−54] Metal uptake can occur by various mechanisms, which were reported to include extracellular accumulation and adsorption–absorption on cell surfaces or precipitation.[49,55]

RESULTS AND DISCUSSION

Uranium Content in Plant Samples along Rio Paguate. The accumulation of U was detected in plant samples collected from the field. Samples were collected along the Rio Paguate either near the abandoned mine wastes (sites 1, 5, and 7) or 5 km away in and near the wetland area (sites 8–10) (Table S1). Among the studied species, the highest U accumulation was found in grass plants. Uranium concentrations in grass root samples were 2.6–18-fold higher (3.1–21.3 mg kg^{-1} U) compared to those in willow and cattail. As for shoots, grass samples had 5.2–24-fold higher (2.6–11.7 mg kg^{-1}) U contents compared to willow and cattail shoots. The variation of U concentrations in grass samples did not show a correlation with the sediments and water properties along the stream bank of Rio Paguate (e.g., water pH, Ca, and U concentrations). However, the highest observed U accumulation in grass roots (21.3 mg kg^{-1}) was at the wetland site, which coincides with the highest U concentration in sediments as measured by Blake et al.[14] This observation is consistent with previous studies where the rhizosphere in wetland sediments naturally contributes to the immobilization of U.[42,56] However, the range of U concentrations in grass roots and shoots are still lower than those reported for other plants studied at various U mine sites.[57,58] Although plant samples collected from the field had detectable U content measured by ICP-MS, it was difficult to use X-ray spectroscopy analyses to understand the mechanisms affecting U accumulation given that the concentrations measured were below the detection limit (<100 mg kg^{-1}). Another limitation is that the effects of plant maturation, the U exposure duration, and the typical seasonal variation of sediment and water properties (e.g., U, Ca, and carbonate concentrations)[14] at the site on the processes of U accumulation in these plants are still unknown. Thus, hydroponic experiments were conducted under laboratory-controlled conditions using *B. juncea*, a hyper-accumulator model plant, to investigate the kinetics of U uptake and

DOI: 10.1021/acs.est.8b02724
Environ. Sci. Technol. 2018, 52, 13089−13098

Table 1. Kinetic Parameters for U Uptake by *Brassica juncea* Roots[a]

U concentration (μg L^{-1})	Ca (mg L^{-1})	V_0 (μg g^{-1} h^{-1})	k_2 (g μg^{-1} h^{-1})	q_e (μg g^{-1})	R^2
30	0	4.44 ± 1.9abcd	0.0103 ± 0.0003a	24 ± 6.3bc	0.9949
100	0	25.94 ± 3.3abc	0.003ab	95.5 ± 5.7abc	0.9888
300	0	29.17 ± 5.9ab	0.0004bc	264.8 ± 29.6a	0.9743
700	0	62.75 ± 5.54a	0.00011 ± 0.00009c	868 ± 344a	0.9527
30	12	0.73 ± 0.15d	0.003 ± 0.001ab	17 ± 0.7c	0.9787
100	12	1.05 ± 0.5d	0.002abc	20 ± 7.8bc	0.9406
300	12	1.82cd	0.00017bc	99.01ab	0.9382
700	12	2.07 ± 0.21bcd	0.00012 ± 0.00002c	109.3 ± 45.7ab	0.9535

[a]The following parameters are represented as the calculated average value with the corresponding standard deviation (SD) for triplicate experiments: the initial uptake rate, V_0 (± SD); the rate constant of pseudo-second-order, k_2 (± SD); and the mass of U per gram of root at equilibrium, q_e (± SD). Different letters indicate significant differences ($p < 0.05$) between different U and Ca treatments in each column as indicated by the Kruskal–Wallis test followed by Dunn's test.

how aqueous Ca and U concentrations at circumneutral pH could affect U bioavailability. Although the mechanisms of U accumulation by *B. juncea* may not be directly transferrable to species from the field, *B. juncea* was used in this study for testing the mechanisms of U bioaccumulation as a research model species.[9,44,45]

Hydroponic Experiments for Uranium Uptake. *B. juncea* was observed in other studies to be able to hyperaccumulate U in the roots but also in the shoots under high U concentrations that have limited environmental relevance for various abandoned mine sites.[7,8,59] In this study, we selected U and Ca concentrations (Table S1) representative of the Rio Paguate surface water concentrations and assessed U uptake in *B. juncea* from carbonate water. The uptake of U by plants was calculated based on changes in aqueous U concentrations over time. The highest U uptake was observed in experiments conducted with no added Ca where aqueous U concentration significantly decreased over time ($p < 0.05$). However, high Ca concentrations showed a significant ($p < 0.05$) inhibitory effect on U uptake from carbonate water (Figures 1 and S2). Fast U uptake was observed with 8% of the total U concentration removed from solution within 20 min of roots exposure to 700 μg L^{-1} U for experiments with both 0 and 12 mg L^{-1} Ca (Figure S2). However, after 2 h, U uptake was 2.2-fold higher in water free of Ca compared to that containing 12 mg L^{-1} Ca. The experiments conducted for 14 days showed that U uptake occurred mainly in the first 24 h for experiments with 0 and 12 mg L^{-1} Ca (Figure 1). For example, at 0 mg L^{-1} Ca, an uptake of 17% was observed for 700 μg L^{-1} U and 47% was observed for 30 μg L^{-1} U. However, only 7–18% of U was removed for experiments with 12 mg L^{-1} Ca, and no measurable uptake was detected in solutions at 240 mg L^{-1} Ca over time. Uranium uptake was limited after 24 h as evidenced by the non-noticeable change in U concentration in the later period of the experiment.

Higher percentages of U uptake (60–80%) were observed within 24 h in a previous study with plants exposed to similar U concentrations as those used in our experiments.[60] However, the pH during the exposure period and water chemistry (i.e., hard elements, carbonates) were not reported. Another study has shown 24% U uptake by sunflowers at pH 7[34] but in the presence of phosphate, which is known to preferentially bind U with respect to the other complexing agents (i.e., carbonates) over a pH range of 4.5–9.[35] Although our study was conducted using different experimental conditions and in the absence of phosphorus in the water, we obtained comparable U uptake (7–18% for experiments with 12 mg L^{-1} Ca), which can be related to the circumneutral pH used in both studies. On the basis of chemical equilibrium analyses (Table S2), UO_2^{2+} should not be predominant, and phosphate- and carbonate-U complexes are neutrally to negatively charged at pH 7.5. The binding of these negative or neutral complexes with plant roots was previously reported to be lower compared to UO_2^{2+},[61,62] most likely because of the negatively charged compounds that compose the vegetal cell walls and membranes.[33,39]

Uranium Accumulation in *Brassica juncea*. Uranium accumulated in *B. juncea* roots, with no detectable root-to-shoot translocation. For example, when exposed to 700 μg L^{-1} U at 0 mg L^{-1} Ca, 924 ± 447 mg kg^{-1} U was measured in the digested samples of plant roots, whereas only 0.7 ± 0.3 mg kg^{-1} U was measured in the shoots (Figure S3). As shown in Figure S3, the content of U in plant roots that was obtained by calculation was found to be significantly similar ($p > 0.05$) to that measured in the digested root samples for both experiments with 0 and 12 mg L^{-1} Ca. It is worth noting that the measured concentrations of U in *B. juncea* roots for experiments with 240 mg L^{-1} Ca correspond to only ∼1% of U uptake, which could not be detected during the measurements of U uptake in solution over time. The undetectable root-to-shoot translocation is consistent with a previous study where the measured U concentration in leaves was ∼1.64 mg kg^{-1} in plants exposed to lower than 6.4 μmol L^{-1} U at pH 7.5.[63] However, at higher U concentrations (>25 μmol L^{-1}, which are seldom observed in the environment), considerable translocation of U to the shoots was typically observed and attributed to the mobility of uranyl-carbonate complexes[33,63] at pH 7.5 compared to uranyl cations formed at pH 4. Future studies should focus on a greater understanding of the effect of Ca and U concentrations on U translocation. In addition, the measured concentrations of U in *B. juncea* roots for experiments with 240 mg L^{-1} Ca (27.4 ± 8.1 mg kg^{-1}) were close to U contents in the grass roots at the wetland site in the Jackpile Mine where plants were exposed to natural Ca concentrations in surface water (7.7–278 mg L^{-1}), similar to our experimental conditions (Table S1).

The initial U and Ca concentrations in the exposure solution significantly ($p < 0.05$) affect the accumulation of U in plant roots (Table S3). For example, when initial U concentrations increased from 30 to 700 μg L^{-1}, U uptake (μg g^{-1}) significantly increased ($p < 0.05$) 36-fold at 0 mg L^{-1} Ca and 8-fold at 12 mg L^{-1} Ca (Table S3). A linear relationship was obtained for experiments using 0 and 12 mg L^{-1} Ca with coefficient of correlation (R^2) values of 0.9866 and 0.89

DOI: 10.1021/acs.est.8b02724
Environ. Sci. Technol. 2018, 52, 13089–13098

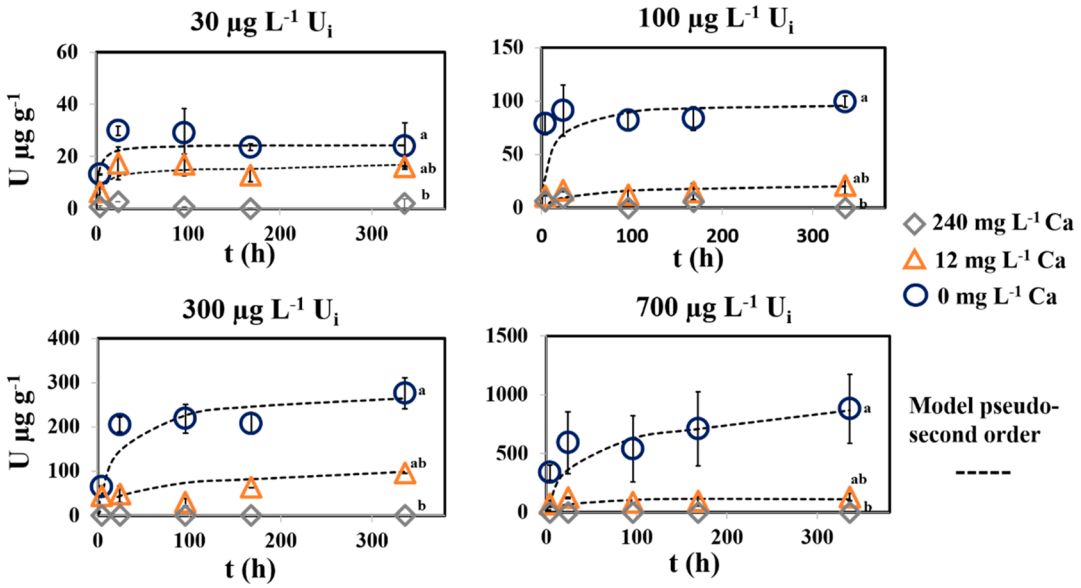

Figure 2. Uranium uptake in plant roots ($\mu g\ g^{-1}$) at different initial U_i and Ca concentrations in solutions containing 1 mM HCO_3^- at pH 7.5. The uptake rate followed a pseudo-second-order kinetic model. The standard deviation was determined from triplicate experiments. Different letters indicate significant difference ($p < 0.05$) in U uptake (as indicated by Kruskal–Wallis test followed by Dunn's test) between solutions with different Ca treatments at the different levels of initial U_i concentration.

respectively (Table S3). These results are in agreement with another study that showed a linear relationship between the accumulation of U in sunflowers and its initial concentration in soil solution.[34]

Kinetic Analyses of Aqueous U. Kinetic analyses were conducted to evaluate the differences in initial uptake rates (V_0) of U into plant roots, as a function of aqueous U and Ca concentrations in the carbonate water at pH 7.5 under environmentally relevant conditions. Significant increase in U uptake rate ($p < 0.05$) was observed when waters contained the highest U concentration (700 $\mu g\ L^{-1}$) with no Ca (Table 1). In all the cases, pseudo-second-order was the most appropriate fitting model (Figure 2) generating R^2 values of ≥0.9382 (Table 1) for the plots of t/q_t versus t, except at 240 mg L^{-1} Ca where no detectable uptake was measured over time. The values of V_0 and q_e were determined following eq 3 and are presented in Table 1 for all U initial concentrations. A high linear relationship ($R^2 = 0.9994$) exists between all the experimental and the calculated values of q_e (Figure S4). The uptake of U by *B. juncea* roots was found to follow pseudo-second-order kinetics, presenting a fast U uptake in the first 24 h of exposure until approaching equilibrium between the remaining aqueous U and the accumulated U in roots (Figure 2). The approaching equilibrium can be observed by the linear relationship between the remaining aqueous U and U uptake for experiments with 0 mg L^{-1} Ca ($R^2 = 0.9931$) and 12 mg L^{-1} Ca ($R^2 = 0.7161$) (Figure S5). The pseudo-second-order model was reported in other studies attributing metal uptake in plants and bacteria to adsorption–absorption mechanisms.[52,53,64,65] These mechanisms were also reported in studies investigating U biological uptake where U adsorption and precipitation were proposed to represent the main mechanisms of U uptake onto root cell walls.[33,60] Gerber et al. attributed the fast phase of U uptake by a Gram-negative bacteria to the biosorption of U onto the cell membrane, which was confirmed by TEM.[66]

The initial uptake rate (V_0) of U was found to be highly affected by Ca concentration in carbonate water at circumneutral pH. The increase of Ca from 0 to 12 mg L^{-1} in carbonate water at pH 7.5 reduced V_0 by at least 6-fold for all initial U concentrations (Table 1). For instance, at 700 $\mu g\ L^{-1}$ U, V_0 significantly decreased ($p < 0.05$) from 62.75 ± 5.54 to 2.07 ± 0.21 $\mu g\ g^{-1}\ h^{-1}$. The inverse relationship between the uptake rate of U and Ca concentration in solution is consistent with the inhibiting effect of Ca on U bioavailability. This effect may be due to the following possibilities: (1) a direct effect of Ca^{2+} on U uptake by inducing a competitive mechanism with UO_2^{2+} or (2) the complexation of UO_2^{2+} with Ca^{2+} and carbonate to form strong ternary Ca–U–CO_3 complexes that are less bioavailable to plants than other aqueous species.

Chemical equilibrium modeling based on the experimental conditions used in this study suggests that the distribution of U aqueous species was greatly affected by the presence of Ca and carbonate at pH 7.5. For instance, in the absence of Ca at 700 $\mu g\ L^{-1}$ U, $(UO_2)_2CO_3(OH)_3^-$ is predicted to highly occur (91.1%) with the presence of 7.6% of binary uranyl-carbonate complexes U–CO_3 (mainly $UO_2(CO_3)_2^{-2}$ and UO_2CO_3) (Table S2). In water containing 12 mg L^{-1} Ca, the fraction of $(UO_2)_2CO_3(OH)_3^-$ decreases to 79% with a simultaneous 12.6% formation of ternary Ca–U–CO_3 (mainly $CaUO_2(CO_3)_3^{-2}$ and $Ca_2UO_2(CO_3)_3$). For experiments with 240 mg L^{-1} Ca, Ca–U–CO_3 aqueous species highly occur (about 99%). Among all exposure solutions, the presence of free UO_2^{2+} was not detected, and only 0.1–4.9% of UO_2–OH were predicted to be present. These observations are consistent with those reported in many other studies.[28,67]

The negligible presence of the positively charged uranyl cations in all solutions suggests that the charge competitive mechanism between U aqueous species and Ca^{2+} uptake likely was not the main reason for U uptake inhibition. Croteau et al. have reported that U does not exclusively use Ca membrane transporter during its bioaccumulation in invertebrates.[28] Alternatively, Ca may exert an indirect effect by decreasing the U bioavailable fraction through the formation of Ca–U–CO_3 complexes. When neutral $Ca_2UO_2(CO_3)_3$ became the dominant species for experiments with 240 mg L^{-1} Ca, U

DOI: 10.1021/acs.est.8b02724
Environ. Sci. Technol. 2018, 52, 13089–13098

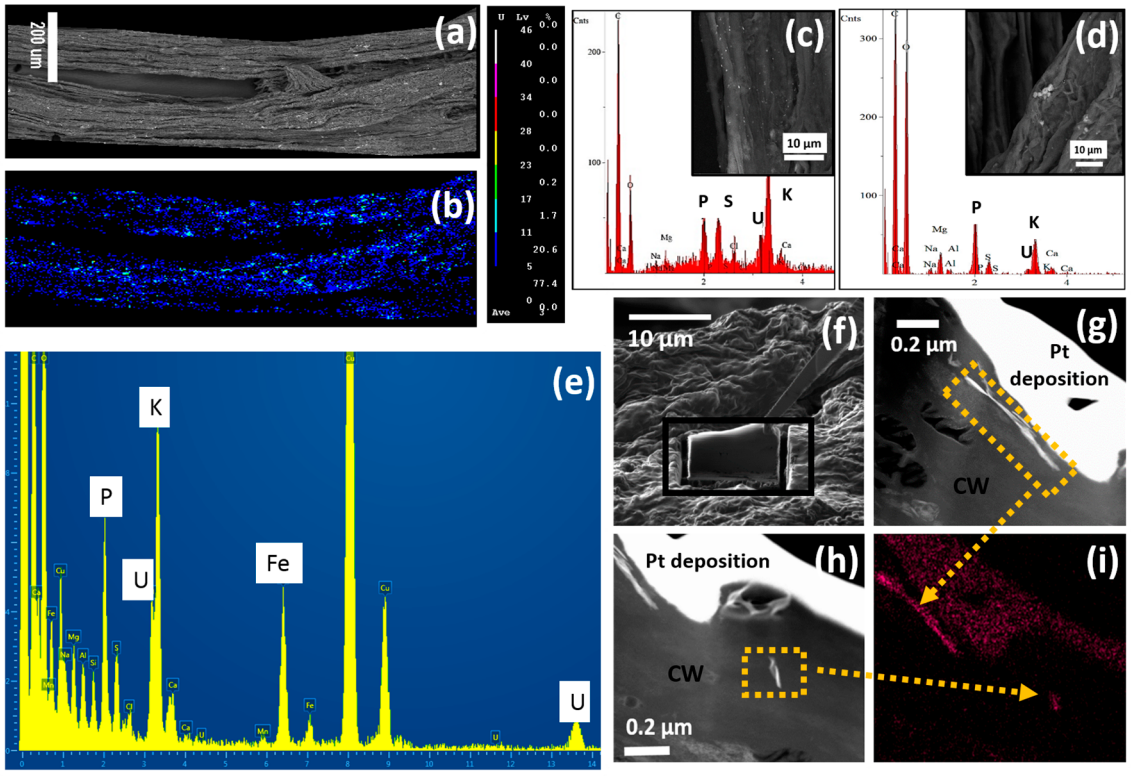

Figure 3. Backscattered electron (BSE) SEM images, microprobe mapping, and energy dispersive spectroscopy (EDS) spectra for root surface in water free of Ca at 700 μg L^{-1} U indicating the accumulation of U on root cell walls and the formation of particles containing U and P: (a) BSE image corresponding to the microprobe mapping; (b) microprobe mapping showing the distribution of U on root surface; (c and d) BSE images and EDS spectra of a cluster of U−P bearing particles; (e) EDS spectra for the FIB cross section across the cell walls (CW) of root surface identifying the co-occurrence of U, P, and Fe in the cell walls; (f) secondary electron (SE) SEM extraction of the FIB section across the cell walls of root surface; (g and h) STEM images of FIB cross section showing U precipitates in the cell wall of root; and (i) STEM X-ray map for U in the FIB cross section confirming U precipitation in the cell wall of epidermal cells.

uptake decreased (Figure S6). This is consistent with the study of Croteau et al., which showed that $UO_2(CO_3)_2^{-2}$ aqueous species represent the best predictor for U uptake rate and suggested that the Ca−U−CO_3 aqueous species are less bioavailable to invertebrates than other U species.[28] In our study, the rate constant of pseudo-second-order k_2 presented a highly linear relationship ($R^2 \geq 0.9486$) with the distribution of U−CO_3 species (Figure S7) as a function of the total U concentration at 0 and 12 mg L^{-1} Ca. When U−CO_3 species predominate, the calculated k_2 in this study (k_2 = 0.0103 ± 0.0003 g μg^{-1} h^{-1}) was found to be higher than those reported in other studies for U uptake by bacteria[68] or for the uptake of other metals by various plants (Table S4).[53,69] Other studies reported that neutral $Ca_2UO_2(CO_3)_3$ can inhibit U toxicity in porcine proximal kidney cells[30] and microbiological U(VI) reduction.[67,70] However, the effect of Ca on U bioavailability in plants through the formation of Ca−U−CO_3 species has been not recognized in the literature. For example, Markich related the mechanisms of U bioaccumulation by macrophyte to a competitive mechanism between Ca^{2+} and UO_2^{2+} and did not consider the influence of uranyl-carbonate species despite their predominance in the exposure media.[21] Thus, the findings presented in this study provide relevant insights about the bioavailability and the effect of U−CO_3 and Ca−U−CO_3 in plants. Further microscopic and spectroscopic analyses were conducted to *B. juncea* roots to better understand the mechanisms of U uptake.

Solid Analysis. The accumulation of U on the surface of plant roots that were exposed to 700 μg L^{-1} U at low Ca concentration (0 and 12 mg L^{-1}) was confirmed by SEM-EDS and electron microprobe X-ray mapping analyses (Figures 3 and S8). Images obtained using SEM−backscattered electron (BSE) show U-bearing particles (0.3−0.7 μm) randomly distributed on the root surface for experiments using 0 mg L^{-1} Ca, which were confirmed by microprobe mapping (Figure 3). The EDS spectra of these particles showed the presence of P, S, U, Ca, and K. These elements have an important structural and functional role in plant tissues.[71] Some clusters of U-bearing particles (~2.2 μm) with similar elemental compositions were also detected on root surfaces. Because of the low accumulated U concentration (<100 mg kg^{-1}) in roots for experiments using 12 mg L^{-1} Ca, fewer clusters of U-bearing particles were detected in these samples (Figure S8).

To identify if U has penetrated the epidermis cells, a FIB section prepared from across the cell walls was analyzed by scanning transmission electron microscopy/energy-dispersive X-ray spectrometry (STEM/EDS) X-ray mapping. Bright precipitates enriched with U were identified in the cell walls (Figure 3). The EDS spectra of these U-bearing precipitates contained P, U, K and Fe (Figure 3). According to previous studies, U could be highly retained on cell walls forming precipitates with endogenous P, especially when the U is not complexed with organic acids.[7,39] Furthermore, the coexistence of a high Fe peak in the same area where U-bearing precipitates (Figure 3) occur can also have implications for

DOI: 10.1021/acs.est.8b02724
Environ. Sci. Technol. 2018, 52, 13089−13098

the mechanisms of U bioaccumulation. For instance, although cell walls are known to contain essential elements like P, K, and Fe, Berthet et al. have shown that U accumulation in plant roots can have significant effect on Fe and P homeostasis.[72]

Other studies have reported that U accumulation mechanisms can differ depending on its aqueous speciation and suggested that U accumulation in root cell walls can be attributed mostly to the following electrostatic interactions: (1) high electrostatic attraction between the positively charged UO_2^{2+} and the cell walls, resulting in high root accumulation with no root-to-shoot translocation, and (2) high electrostatic repulsion between the negatively charged uranyl-carbonate and the cell walls, resulting in lower U root accumulation with higher root-to-shoot translocation.[33,39] Plants exposed to uranyl-carbonate (100 μM U in solutions with 10 mM carbonate at pH 7) by Laurette et al. have shown U entrapped with P in the cell walls of leaves, but the accumulation sites for U in the roots could not be detected.[33] However, in that study, plants were exposed to 100 times higher U concentration than in this study. Thus, a direct comparison between the results from this study and those from Laurette et al. is not possible because U toxicity may also contribute to the uptake mechanisms at higher concentrations.[40] Future investigations should assess the impact of U concentrations on uranyl-carbonate uptake in the root and root-to-shoot translocation.

Although other studies have reported that electrostatic repulsion occurs between uranyl-carbonate complexes and the root cell walls, our study suggests that the exposure of plants to negatively charged uranyl-carbonate can still lead to the accumulation of U on the cell walls of roots. However, the surface complex form in which U was bound and accumulated in the roots is not yet identified or confirmed. The spectroscopic and microscopic results of this study agree with observations made in a study by Gorman-Lewis et al. in which U was found to be adsorbed on the negatively charged bacterial surface after being exposed to the negatively charged uranyl-carbonate complexes.[73] More information is necessary to understand the specific mechanism affecting the interaction and the accumulation of negatively charged U aqueous species in the roots.

Environmental Implications. Uranium uptake by *B. juncea* was found to be greatly affected by Ca in carbonate circumneutral water over a range of environmentally relevant U concentrations. The effect of Ca on U bioavailability was assessed as a function of U speciation in the presence of uranyl-carbonate and ternary uranyl-calcium-carbonate aqueous species, unlike most previous studies, which have focused on investigating solutions in which UO_2^{2+} are predominant.[21,74,75] Kinetic analyses indicate that higher uptake rates are obtained when uranyl-carbonate complexes are present in water. However, the U uptake in plants was inhibited in the presence of Ca and carbonate solutions used in this study, likely due to interactions with neutrally charged ternary uranyl-calcium-carbonate complexes. Given the crucial physiological role of Ca^{2+} in cells, more information is necessary to assess if Ca^{2+} ions affect the uptake of uranyl-carbonate complexes (i.e., Ca^{2+} channels and other membrane proteins). A rapid equilibrium following a pseudo-second-order approach was observed for U in solution at low Ca concentrations (e.g., lower than 12 mg L^{-1} Ca). This is a relevant observation that has implications in semiarid environments characteristic of the southwestern United States in which short rain events can enhance U dissolution[14] and thus U exposure to plant roots. Analyses conducted with STEM and SEM/EDS detected U precipitates (U−P−K-bearing minerals) on the root cell walls after plants were reacted under the conditions selected for this study. The detection of these U-bearing precipitates on root cell walls suggests that negatively charged uranyl-carbonate complexes can interact with the negatively charged cell wall components (e.g., phosphate). Further investigations are necessary to understand how these insoluble U phases could affect the mechanisms of U toxicity in plants. The accumulation of U in plants is relevant as an exposure pathway or as a potential remediation alternative in mining sites. Therefore, more research should focus on better understanding the mechanisms that affect U uptake at environmentally relevant conditions, especially as these relate to the following aspects: (1) determining in which chemical form U surface complexes bind to the root cell walls in carbonate water at weakly basic pH and (2) the influence of U and Ca concentrations on the accumulation and root-to-shoot translocation of U for plants exposed to uranyl-carbonate complexes.

■ ASSOCIATED CONTENT

Supporting Information

The Supporting Information is available free of charge on the ACS Publications website at DOI: 10.1021/acs.est.8b02724.

Additional materials and methods, five additional tables (Tables S1−S5), and eight additional figures (Figures S1−S8) (PDF)

■ AUTHOR INFORMATION

Corresponding Authors

*Phone: (001) (505) 277-0870; fax: (001) (505) 277-1918; e-mail: jcerrato@unm.edu.

*Phone: (001) (505) 582-1362; e-mail: elhayek@unm.edu.

ORCID

Lucia Rodriguez-Freire: 0000-0003-1296-0001

José M. Cerrato: 0000-0002-2473-6376

Notes

The authors declare no competing financial interest.

■ ACKNOWLEDGMENTS

Funding for this research was provided by the National Science Foundation (Grants NM EPSCoR #IIA-1301346, CREST 1345169, and CAREER 1652619), the National Institute of Health Centers of Excellence on Environmental Health Disparities Research (Grant Numbers 1-P50-ES-026102-01 and US-EPA 836157-01), and the National Institute of Environmental Health Sciences Superfund Research Program (Award 1 P42 ES025589). Any opinions, findings, and conclusions or recommendations expressed in this publication are those of the author(s) and do not necessarily reflect the views of the National Science Foundation. Electron microprobe, focused ion beam sample preparation, and transmission electron microscopy were performed in the Electron Microbeam Analysis Facility, Department of Earth and Planetary Sciences and Institute of Meteoritics, University of New Mexico, a facility supported by the State of New Mexico, NASA, and the National Science Foundation. Any use of trade, firm, or product names is for descriptive purposes only and does not imply endorsement by the U.S. Government. All data

DOI: 10.1021/acs.est.8b02724
Environ. Sci. Technol. 2018, 52, 13089−13098

generated or analyzed during this study are included in the main text of this publication and in the supporting information.

REFERENCES

(1) Winde, F.; Erasmus, E.; Geipel, G. Uranium contaminated drinking water linked to leukaemia-Revisiting a case study from South Africa taking alternative exposure pathways into account. *Sci. Total Environ.* **2017**, *574*, 400−421.

(2) Ferrari, C. R.; Do Nascimento, H. D. A. F.; Rodgher, S.; Almeida, T.; Bruschi, A. L.; Do Nascimento, M. R. L.; Bonifácio, R. L. Effects of the discharge of uranium mining effluents on the water quality of the reservoir: An integrative chemical and ecotoxicological assessment. *Sci. Rep.* **2017**, *7* (1), 13919.

(3) Avasarala, S.; Lichtner, P. C.; Ali, A.-M. S.; González-Pinzón, R.; Blake, J. M.; Cerrato, J. M. Reactive transport of U and V from abandoned uranium mine wastes. *Environ. Sci. Technol.* **2017**, *51* (21), 12385−12393.

(4) Schreck, E.; Dappe, V.; Sarret, G.; Sobanska, S.; Nowak, D.; Nowak, J.; Stefaniak, E. A.; Magnin, V.; Ranieri, V.; Dumat, C. Foliar or root exposures to smelter particles: Consequences for lead compartmentalization and speciation in plant leaves. *Sci. Total Environ.* **2014**, *476*−*477*, 667−676.

(5) El Hayek, E.; El Samrani, A.; Lartiges, B.; Kazpard, V.; Benoit, M.; Munoz, M. Potential of *Opuntia ficus-indica* for air pollution biomonitoring: A lead isotopic study. *Environ. Sci. Pollut. Res.* **2015**, *22* (22), 17799−17809.

(6) El Hayek, E.; El Samrani, A.; Lartiges, B.; Kazpard, V.; Aigouy, T. Lead bioaccumulation in *Opuntia ficus-indica* following foliar or root exposure to lead-bearing apatite. *Environ. Pollut.* **2017**, *220*, 779−787.

(7) Huang, J. W.; Blaylock, M. J.; Kapulnik, Y.; Ensley, B. D. Phytoremediation of uranium-contaminated soils: Role of organic acids in triggering uranium hyperaccumulation in plants. *Environ. Sci. Technol.* **1998**, *32* (13), 2004−2008.

(8) Duquène, L.; Vandenhove, H.; Tack, F.; Meers, E.; Baeten, J.; Wannijn, J. Enhanced phytoextraction of uranium and selected heavy metals by Indian mustard and ryegrass using biodegradable soil amendments. *Sci. Total Environ.* **2009**, *407* (5), 1496−1505.

(9) Eapen, S.; Suseelan, K. N.; Tivarekar, S.; Kotwal, S. A.; Mitra, R. Potential for rhizofiltration of uranium using hairy root cultures of *Brassica juncea* and *Chenopodium amaranticolor*. *Environ. Res.* **2003**, *91* (2), 127−133.

(10) Moench, R. H.; Schlee, J. S. *Geology and uranium deposits of the Laguna district*; US Government Printing Office: NM, 1967.

(11) Nash, J. T. Uranium deposits in the Jackpile Sandstone, New Mexico. *Econ. Geol. Bull. Soc. Econ. Geol.* **1968**, *63*, 737−750.

(12) U. S. Geological Survey, 08349800 Rio Paguate below Jackpile Mine near Laguna, NM; https://waterdata.usgs.gov/nwis/inventory?agency_code=USGS&site_no=08349800, 2017 (accessed Januray 14, 2017).

(13) USEPA. *Technical report on technologically enhanced naturally occurring radioactive materials from uranium mining volume 1: Mining and reclamation background*; U.S. Environmental Protection Agency, Office of Radiation and Indoor Air; EPA 402-R-08-005, 2008.

(14) Blake, J. M.; De Vore, C. L.; Avasarala, S.; Ali, A.-M.; Roldan, C.; Bowers, F.; Spilde, M. N.; Artyushkova, K.; Kirk, M. F.; Peterson, E.; Rodriguez-Freire, L.; Cerrato, J. Uranium mobility and accumulation along the Rio Paguate, Jackpile Mine in Laguna Pueblo, New Mexico. *Environ. Sci. Process. Impacts* **2017**, *19*, 605−621.

(15) Goulet, R. R.; Fortin, C.; Spry, D. Uranium. In *Homeostasis and toxicology of non-essential metals*; Wood, C. M., Farrel, A. P., Brauner, C. J., Eds.; Academic Press, 2012; pp 391−428.

(16) Markich, S. J.; Twining, J. R. Radioecology of tropical freshwater ecosystems: Mechanisms and kinetics of bioaccumulation and the importance of water chemistry. In *Tropical Radioecology*; Amsterdam, 2012; pp 233−82.

(17) Trenfield, M. A.; McDonald, S.; Kovacs, K.; Lesher, E. K.; Pringle, J. M.; Markich, S. J.; Ng, J. C.; Noller, B.; Brown, P. L.; Van Dam, R. A. Dissolved organic carbon reduces uranium bioavailability and toxicity. 1. Characterization of an aquatic fulvic acid and its complexation with uranium [VI]. *Environ. Sci. Technol.* **2011**, *45* (7), 3075−3081.

(18) Fortin, C.; Denison, F. H.; Garnier-Laplace, J. Metal-phytoplankton interactions: modeling the effect of competing ions ($H^+$$Ca^{2+}$ and Mg^{2+}) on uranium uptake. *Environ. Toxicol. Chem.* **2007**, *26*, 242−248.

(19) Tran, D.; Massabuau, J. C.; Garnier-Laplace, J. Effect of carbon dioxide on uranium bioaccumulation in the freshwater clam *Corbicula fluminea*. *Environ. Toxicol. Chem.* **2004**, *23*, 739−47.

(20) Campbell, P. G. C. Interactions between trace metals and aquatic organisms: A critique of the free-ion activity model. In *Metal Speciation and Bioavailability in Aquatic Systems*; Tessier, A., Turner, D. R., Eds.; John Wiley and Sons: New York, 1995; pp 45−102.

(21) Markich, S. J. Water hardness reduces the accumulation and toxicity of uranium in a freshwater macrophyte (*Ceratophyllum demersum*). *Sci. Total Environ.* **2013**, *443*, 582−589.

(22) Du, L.; Feng, X.; Huang, Z.; Liu, B.; Jin, Y.; Fang, Z.; Zhang, D.; Liu, N.; Wang, R.; Xia, C. The effect of U speciation in cultivation solution on the uptake of U by variant *Sedum alfredii*. *Environ. Sci. Pollut. Res.* **2016**, *23* (10), 9964−9971.

(23) Taylor, H. E.; Peart, D. B.; Antweiler, R. C.; Brinton, T. I.; Campbell, W. L.; Garbarino, J. R.; Roth, D. A.; Hart, R. J.; Averett, R. C. Data from synoptic water-quality studies on the Colorado river in the grand canyon, Arizona, November 1990 and June 1991. USGS Open-File Report 96-614; 1996.

(24) Dong, W.; Brooks, S. C. Determination of the formation constants of ternary complexes of uranyl and carbonate with alkaline earth metals ($Mg^{2+}$$Ca^{2+}$$Sr^{2+}$ and Ba^{2+}) using anion exchange method. *Environ. Sci. Technol.* **2006**, *40* (15), 4689−4695.

(25) Yan, S.; Boyanov, M. I.; Mishra, B.; Kemner, K. M.; O'Loughlin, E. J. U(VI) Reduction by biogenic and abiotic hydroxycarbonate green rusts: Impacts on U(IV) Speciation and stability over time. *Environ. Sci. Technol.* **2018**, *52*, 4601−4609.

(26) Wen, H.; Pan, Z.; Giammar, D.; Li, L. Enhanced uranium immobilization by phosphate amendment under variable geochemical and flow conditions: Insights from reactive transport modeling. *Environ. Sci. Technol.* **2018**, *52*, 5841−5850.

(27) Riethmuller, N.; Markich, S.; Van Dam, R.; Parry, D. Effects of water hardness and alkalinity on the toxicity of uranium to a tropical freshwater hydra (*Hydra viridissima*). *Biomarkers* **2001**, *6*, 45−51.

(28) Croteau, M. N.; Fuller, C. C.; Cain, D. J.; Campbell, K. M.; Aiken, G. Biogeochemical controls of uranium bioavailability from the dissolved phase in natural freshwaters. *Environ. Sci. Technol.* **2016**, *50* (15), 8120−8127.

(29) Muller, D.; Houpert, P.; Cambar, J.; Henge-Napoli, M. H. Role of the sodium-dependent phosphate co-transporters and of the phosphate complexes of uranyl in the cytotoxicity of uranium in LLC-PK(1) cells. *Toxicol. Appl. Pharmacol.* **2006**, *214*, 166−77.

(30) Carrière, M.; Avoscan, L.; Collins, R.; Carrot, F.; Khodja, H.; Ansoborlo, E.; Gouget, B. Influence of uranium speciation on normal rat kidney (NRK-52E) proximal cell cytotoxicity. *Chem. Res. Toxicol.* **2004**, *17* (3), 446−452.

(31) Prat, O.; Vercouter, T.; Ansoborlo, E.; Fichet, P.; Perret, P.; Kurttio, P.; Salonen, L. Uranium speciation in drinking water from drilled wells in Southern Finland and its potential links to health effects. *Environ. Sci. Technol.* **2009**, *43* (10), 3941−3946.

(32) Goulet, R. R.; Thompson, P. A.; Serben, K. C.; Eickhoff, C. V. Impact of environmentally based chemical hardness on uranium speciation and toxicity in six aquatic species. *Environ. Toxicol. Chem.* **2015**, *34* (3), 562−574.

(33) Laurette, J.; Larue, C.; Mariet, C.; Brisset, F.; Khodja, H.; Bourguignon, J.; Carrière, M. Influence of uranium speciation on its accumulation and translocation in three plant species: Oilseed rape, sunflower and wheat. *Environ. Exp. Bot.* **2012**, *77*, 96−107.

(34) Rodríguez, P. B.; Tomé, F. V.; Fernández, M. P.; Lozano, J. C. Linearity assumption in soil-to-plant transfer factors of natural uranium and radium in *Helianthus annuus L. Sci. Total Environ.* **2006**, *361* (1−3), 1−7.

DOI: 10.1021/acs.est.8b02724
Environ. Sci. Technol. 2018, 52, 13089−13098

(35) Ebbs, S. D.; Brady, D. J.; Kochian, L. V. Role of uranium speciation in the uptake and translocation of uranium by plants. *J. Exp. Bot.* **1998**, *49* (324), 1183−1190.
(36) Boghi, A.; Roose, T.; Kirk, G. J. D. A model of uranium uptake by plant roots allowing for root-induced changes in the soil. *Environ. Sci. Technol.* **2018**, *52* (6), 3536−3545.
(37) Edayilam, N.; Montgomery, D. A.; Ferguson, B. O.; Maroli, A. S.; Martinez, N.; Powell, B. A.; Tharayil, N. Phosphorus stress-induced changes in plant root exudation could potentially facilitate uranium mobilization from stable mineral forms. *Environ. Sci. Technol.* **2018**, *52* (14), 7652−7662.
(38) Saenen, E.; Horemans, N.; Vanhoudt, N.; Vandenhove, H.; Biermans, G.; Van Hees, M.; Wannijn, J.; Vangronsveld, J.; Cuypers, A. Effects of pH on uranium uptake and oxidative stress responses induced in *Arabidopsis thaliana*. *Environ. Toxicol. Chem.* **2013**, *32* (9), 2125−2133.
(39) Laurette, J.; Larue, C.; Llorens, I.; Jaillard, D.; Jouneau, P. H.; Bourguignon, J.; Carrière, M. Speciation of uranium in plants upon root accumulation and root-to-shoot translocation: A XAS and TEM study. *Environ. Exp. Bot.* **2012**, *77*, 87−95.
(40) Misson, J.; Henner, P.; Morello, M.; Floriani, M.; Wu, T. D.; Guerquin-Kern, J. L.; Fevrier, L. Use of phosphate to avoid uranium toxicity in *Arabidopsis thaliana* leads to alterations of morphological and physiological responses regulated by phosphate availability. *Environ. Exp. Bot.* **2009**, *67*, 353−62.
(41) Gunther, A.; Bernhard, G.; Geipel, G.; Reich, T.; Rossberg, A.; Nitsche, H. Uranium speciation in plants. *Radiochim. Acta* **2003**, *91*, 319−328.
(42) Li, D.; Kaplan, D. I.; Chang, H. S.; Seaman, J. C.; Jaffé, P. R.; Koster Van Groos, P.; Scheckel, K. G.; Segre, C. U.; Chen, N.; Jiang, D. T.; Newville, M.; Lanzirotti, A. Spectroscopic evidence of uranium immobilization in acidic wetlands by natural organic matter and plant roots. *Environ. Sci. Technol.* **2015**, *49* (5), 2823−2832.
(43) Chang, H. S.; Buettner, S. W.; Seaman, J. C.; Jaffé, P. R.; Koster Van Groos, P. G.; Li, D.; Peacock, A. D.; Scheckel, K. G.; Kaplan, D. I. Uranium immobilization in an iron-rich rhizosphere of a native wetland plant from the savannah river site under reducing conditions. *Environ. Sci. Technol.* **2014**, *48* (16), 9270−9278.
(44) Straczek, A.; Duquene, L.; Wegrzynek, D.; Chinea-Cano, E.; Wannijn, J.; Navez, J.; Vandenhove, H. Differences in U root-to-shoot translocation between plant species explained by U distribution in roots. *J. Environ. Radioact.* **2010**, *101* (3), 258−266.
(45) Qi, F.; Zha, Z.; Du, L.; Feng, X.; Wang, D.; Zhang, D.; Fang, Z.; Ma, L.; Jin, Y.; Xia, C. Impact of mixed low-molecular-weight organic acids on uranium accumulation and distribution in a variant of mustard (*Brassica juncea* var. *tumida*). *J. Radioanal. Nucl. Chem.* **2014**, *302* (1), 149−159.
(46) Gustafsson, J. P. Visual MINTEQ ver. 3.1. https://vminteq.lwr.kth.se/download/.
(47) Hu, S.; Lu, Y.; Peng, L.; Wang, P.; Zhu, M.; Dohnalkova, A. C.; Chen, H.; Lin, Z.; Dang, Z.; Shi, Z. Coupled kinetics of ferrihydrite transformation and As (V) sequestration under the effect of humic acids: A mechanistic and quantitative Study. *Environ. Sci. Technol.* **2018**, *52* (V), 11632−11641.
(48) Le Menn, N.; Marchand, S.; De Revel, G.; Demarville, D.; Laborde, D.; Marchal, R. N,S,O-Heterocycles in aged champagne reserve wines and correlation with free amino acid concentrations. *J. Agric. Food Chem.* **2017**, *65* (11), 2345−2356.
(49) Keskinkan, O.; Goksu, M. Z. L.; Basibuyuk, M.; Forster, C. F. Heavy metal adsorption properties of a submerged aquatic plant (*Ceratophyllum demersum*). *Bioresour. Technol.* **2004**, *92* (2), 197−200.
(50) Hossain, A.; Bhattacharyya, S. R.; Aditya, G. Biosorption of cadmium by waste shell dust of fresh water mussel *lamellidens marginalis*Implications for metal bioremediation. *ACS Sustainable Chem. Eng.* **2015**, *3* (1), 1−8.
(51) Bai, H. J.; Zhang, Z. M.; Yang, G. E.; Li, B. Z. Bioremediation of cadmium by growing *Rhodobacter sphaeroides* Kinetic characteristic and mechanism studies. *Bioresour. Technol.* **2008**, *99* (16), 7716−7722.
(52) Reddad, Z.; Gerente, C.; Andres, Y.; Le cloirec, P. Adsorption of several metal ions onto a low-cost biosorbent: Kinetic and equilibrium studies. *Environ. Sci. Technol.* **2002**, *36*, 2067−2073.
(53) Maleva, M. G.; Malec, P.; Prasad, M. N. V.; Strzałka, K. Kinetics of nickel bioaccumulation and its relevance to selected cellular processes in leaves of *Elodea canadensis* during short-term exposure. *Protoplasma* **2016**, *253* (2), 543−551.
(54) Limcharoensuk, T.; Sooksawat, N.; Sumarnrote, A.; Awutpet, T.; Kruatrachue, M.; Pokethitiyook, P.; Auesukaree, C. Bioaccumulation and biosorption of Cd^{2+} and Zn^{2+} by bacteria isolated from a zinc mine in Thailand. *Ecotoxicol. Environ. Saf.* **2015**, *122*, 322−330.
(55) Veglio, F.; Beolchini, F. Removal of heavy metal ions by biosorption: A review. *Hydrometallurgy* **1997**, *44*, 301−316.
(56) Kaplan, D. I.; Xu, C.; Huang, S.; Lin, Y.; Tolić, N.; Roscioli-Johnson, K. M.; Santschi, P. H.; Jaffé, P. R. Unique organic matter and microbial properties in the rhizosphere of a wetland soil. *Environ. Sci. Technol.* **2016**, *50* (8), 4169−4177.
(57) Butler, A. D.; Wynter, M.; Medina, V. F.; Bednar, A. J. Depleted uranium toxicity, accumulation, and uptake in *Cynodon dactylon* (*Bermuda*) and *Aristida purpurea* (*Purple Threeawn*). *Bull. Environ. Contam. Toxicol.* **2016**, *96* (6), 714−719.
(58) Favas, P. J. C.; Pratas, J.; Mitra, S.; Sarkar, S. K.; Venkatachalam, P. Biogeochemistry of uranium in the soil-plant and water-plant systems in an old uranium mine. *Sci. Total Environ.* **2016**, *568*, 350−368.
(59) Chang, P.; Kim, K. W.; Yoshida, S.; Kim, S. Y. Uranium accumulation of crop plants enhanced by citric acid. *Environ. Geochem. Health* **2005**, *27* (5−6), 529−538.
(60) Lee, M.; Yang, M. Rhizofiltration using sunflower (*Helianthus annuus L*) and bean (*Phaseolus vulgaris L* var. *vulgaris*) to remediate uranium contaminated groundwater. *J. Hazard. Mater.* **2010**, *173* (1−3), 589−596.
(61) Dushenkov, S.; Vasudev, D.; Kapulnik, Y.; Gleba, D.; Fleisher, D.; Ting, K. C.; Ensley, B. Removal of uranium from water using terrestrial plants. *Environ. Sci. Technol.* **1997**, *31* (12), 3468−3474.
(62) Yang, M.; Jawitz, J. W.; Lee, M. Uranium and cesium accumulation in bean (*Phaseolus vulgaris L* var. *vulgaris*) and its potential for uranium rhizofiltration. *J. Environ. Radioact.* **2015**, *140*, 42−49.
(63) Saenen, E.; Horemans, N.; Vanhoudt, N.; Vandenhove, H.; Biermans, G.; Van Hees, M.; Wannijn, J.; Vangronsveld, J.; Cuypers, A. The pH strongly influences the uranium-induced effects on the photosynthetic apparatus of *Arabidopsis thaliana* plants. *Plant Physiol. Biochem.* **2014**, *82*, 254−261.
(64) Vijayaraghavan, K.; Arun, M.; Joshi, U. M.; Balasubramanian, R. Biosorption of As (V) onto the shells of the crab (*Portunus sanguinolentus*): Equilibrium and kinetic Studies. *Ind. Eng. Chem. Res.* **2009**, *48*, 3589−3594.
(65) Mikutta, R.; Baumgärtner, A.; Schippers, A.; Haumaier, L.; Guggenberger, G. Extracellular polymeric substances from bacillus subtilis associated with minerals modify the extent and rate of heavy metal sorption. *Environ. Sci. Technol.* **2012**, *46* (7), 3866−3873.
(66) Gerber, U.; Zirnstein, I.; Krawczyk-Bärsch, E.; Lünsdorf, H.; Arnold, T.; Merroun, M. L. Combined use of flow cytometry and microscopy to study the interactions between the gram-negative betaproteobacterium *Acidovorax facilis* and uranium (VI). *J. Hazard. Mater.* **2016**, *317*, 127−134.
(67) Brooks, S. C.; Fredrickson, J. k.; Carroll, S. L.; Kennedy, D. w.; Zachara, J. M.; Plymale, A. E.; Kelly, S. D.; Kemner, K. M.; Fendorf, S. Inhibition of bacterial U (VI) reduction by calcium. *Environ. Sci. Technol.* **2003**, *37* (9), 1850−1858.
(68) Xie, S.; Yang, J.; Chen, C.; Zhang, X.; Wang, Q.; Zhang, C. Study on biosorption kinetics and thermodynamics of uranium by *Citrobacter freudii*. *J. Environ. Radioact.* **2008**, *99* (1), 126−133.
(69) Keskinkan, O.; Goksu, M. Z. L.; Basibuyuk, M.; Forster, C. F. Heavy metal adsorption properties of a submerged aquatic plant

DOI: 10.1021/acs.est.8b02724
Environ. Sci. Technol. 2018, 52, 13089−13098

(*Ceratophyllum demersum*). *Bioresour. Technol.* **2004**, *92* (2), 197−200.
(70) Stewart, B. D.; Amos, R. T.; Fendorf, S. Effect of uranium (VI) speciation on simultaneous microbial reduction of uranium (VI) and iron (III). *J. Environ. Qual.* **2011**, *40* (1), 90.
(71) George, E. F.; Hall, M. A.; De Klerk, G. J. *Plant propagation by tissue culture*, 3rd ed.; 2008; pp 65−113.
(72) Berthet, S.; Villiers, F.; Alban, C.; Serre, N. B. C.; Martin-Laffon, J.; Figuet, S.; Boisson, A. M.; Bligny, R.; Kuntz, M.; Finazzi, G.; Ravanel, S.; Bourguignon, J. *Arabidopsis thaliana* plants challenged with uranium reveal new insights into iron and phosphate homeostasis. *New Phytol.* **2018**, *217* (2), 657−670.
(73) Gorman-Lewis, D.; Elias, P. E.; Fein, J. B. Adsorption of aqueous uranyl complexes onto *Bacillus subtilis* Cells. *Environ. Sci. Technol.* **2005**, *39* (13), 4906−4912.
(74) Soudek, P.; Petrova, T.; Benesova, D.; Dvorakova, M.; Vanek, T. Uranium uptake by hydroponically cultivated crop plants. *J. Environ. Radioact.* **2011**, *102* (6), 598−604.
(75) Soudek, P.; Petrová, Š.; Buzek, M.; Lhotský, O.; Vaněk, T. Uranium uptake in *Nicotiana sp* under hydroponic conditions. *J. Geochem. Explor.* **2014**, *142*, 130−137.

DOI: 10.1021/acs.est.8b02724
Environ. Sci. Technol. 2018, 52, 13089−13098